PREPRINT UCRL- 79793

CONF-770945--1

Lawrence Livermore Laboratory

DIAGNOSTICS DEVELOPMENTS AND APPLICATIONS FOR LASER FUSION EXPERIMENTS

Lamar W. Coleman

September 2, 1977

This paper was prepared for presentation at the 11th European Conference on Laser Interaction with Matter, Oxford, England, September 19-23, 1977

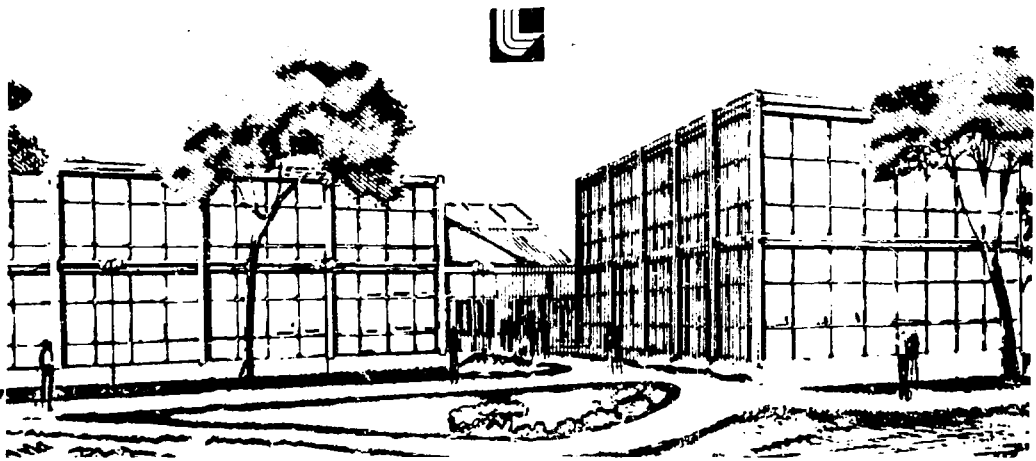

11th European Conference on Laser Interaction With Matter
Oxford, England
19-23 September 1977

Diagnostics Developments and Applications for Laser Fusion Experiments*

Lamar W. Coleman

Lawrence Livermore Laboratory
University of California
Livermore, California 94550

ABSTRACT

Some diagnostics techniques applied to current laser fusion target experiments are reviewed. Specifically, holographic interferometry of target plasmas, coded aperture imaging of thermonuclear alpha-particles and neutron energy spectrum measurements are discussed.

*Work performed under the auspices of the U. S. Energy Research and Development Administration under contract No. W-7405-Eng-48.

Diagnostics Developments and Applications for Laser Fusion Experiments

Introduction

Diagnostics techniques applied to current laser fusion target experiments must in general provide temporal and spatial resolutions on picosecond and micron scales, respectively, in order to provide detailed data on the processes under study. Three high-resolution diagnostics techniques, holographic interferometry of target plasmas, coded aperture imaging of thermonuclear α-particles, and neutron time of flight spectral measurements, all in current use on experiments at Livermore, are discussed (Figure 1)

Plasma Interferometry

The measurement of the electron density distribution in laser-produced plasmas is important in determining the details of the processes occurring during the interaction of the intense laser light pulse with the target plasma.[1,2] A high resolution holographic interferometry system utilizing the fourth-harmonic of the Nd laser pulse for probing the plasma has been developed.[3] Figure 2 shows the scheme employed at the Janus laser facility for the generation of the synchronous, 15 psec duration fourth-harmonic probing pulse. Figure 3 shows the details of the holographic interferometer as installed in the Janus target chamber. This system is capable of providing 1 μm spatial resolution. Figure 4 is interferogram obtained upon 1.06 μm irradiation of a 41 μm diameter glass microsphere irradiated with an intensity of 10^{14}w/cm^2. The probe pulse was adjusted so that this interferogram was obtained at the peak of the 30 psec heating pulse. The plot on the right of Figure 4 shows the Abel inverted on-axis electron density distribution. The result clearly displays a steepened profile, with a scale length of about 1.5 μm, and a maximum measured electron density beyond critical. Figure 5 is an interferogram obtained on a flat disk target at 10^{14}w/cm^2. This result shows evidence of large scale cavity formation, small scale surface rippling, and apparently faster contour velocities on axis indicated by increased fringe smearing.

Coded Aperture Alpha Particle Imaging

The Fresnel zone plate coded aperture technique has been employed to obtain images of the alpha particle emission region in compressed laser fusion targets.[4] Figure 6 outlines the two step shadowcasting and reconstruction scheme used to obtain tomographic images via the zone plate technique. Figure 7 schematically depicts the specific arrangement used for the alpha particle measurements. The alpha particles are recorded in a cellulose nitrate track detector. The combination of an appropriate filter and careful etching procedures for the cellulose nitrate ensures that the recorded pattern is due to the thermonuclear alpha particles, as summarized in Figure 8. Figure 9 is a photograph of the alpha particle produced zone-plate shadowgraph as recorded on the (etched) cellulose nitrate for a target compression experiment conducted at Argus. The target was an 86 μm, D-T filled (1.6 mg/cm^3) glass microsphere irradiated from two sides with 2.4 x 10^{12} watts in a 50 psec FWHM pulse. The neutron yield was 3 x 10^8. Figure 10 shows the reduced data obtained from the reconstructed image. The alpha particle emission region is uniform in shape and has an extent of 27 μm on the average. Spatial resolution of this technique is 10 μm.

Neutron Spectral Measurements

Determination of the energy spectrum of the neutrons emitted from a compressed fusion target provides information on the production mechanism and the reaction temperature. Neutron spectral measurements at the Argus Nd laser facility are made with the time-of-flight spectrometer shown in Figure 11.[5]. Figure 12 summarizes the steps in the data analysis process to obtain the reacting ion temperature. Figure 13 is an example of reduced energy spectrum data obtained on a 7 x 10^8 yield target shot. The target in this case was an 87 μm diameter D-T filled microsphere (2.3 mg/cm^3) irradiated with 2.5 TW (38 psec FWHM pulse). The error bars on each point represent the statistical uncertainty in each resolution interval based on the number of neutrons detected. Figure 14 summarizes results obtained on several Argus shots. Typical ion reaction temperatures measured are in the 5-6 KeV range.

A new, higher resolution, neutron time-of-flight system is being implemented for higher yield Shiva experiments. The capabilities of the Argus and Shiva spectrometers are compared in Figure 15.

Figure 16 summarizes the present status of our high resolution laser fusion diagnostic capabilities over a wide range of measurements, including those discussed above as well as others required for the detailed study of laser fusion experiments.

Acknowledgements

The holographic interferometry has been developed and applied by D. T. Attwood. N. M. Ceglio is responsible for the zone plate imaging work, and R. A. Lerche has performed the neutron spectrometry.

References

1. Estabrook, K. G. Valeo, E. J. and Kruer, W. L., Phys. Fluids, 18, 9, Sept. 1975, p. 1151-1159.

2. Lee, K., Forslund, D. W., Kindel, J. M. and Lindman, E. L., Phys. Fluids, 20, 1, January 1977, pp. 51-54.

3. D. T. Attwood, to be published in Proc. 12th Int'l. Cong. on High Speed Photography. (August, 1976, Toronto). UCRL-77744.

4. Ceglio, N. M. and Coleman, L. W., Phys. Rev. Lett. 39, 1, July 4, 1977, pp. 20-24.

5. Lerche, R. A., Coleman, L. W. Boughton, J. W., Speck, D. R. and Storm, E. K., Bull. Am. Phys. Soc., 21, 9, October 1976, p. 1190. UCRL-78430.

Figure Captions

Fig. 1. Topics included in the paper and the principal investigators.

Fig. 2. U. V. Holographic Interferometer Probe Pulse Optics set up at Janus.

Fig. 3. U. V. Holographic Interferometer Target Chamber Set up at Janus.

Fig. 4. Interferometry result on 41 μm diameter microsphere at Janus.

Fig. 5. Interferogram of irradiated flat disk target.

Fig. 6. Principles of zone plate coded imaging.

Fig. 7. Zone Plate coded Imaging of α-Particles from Laser compressed targets.

Fig. 8. Logic for Radiation Discrimination in α-imaging experiments.

Fig. 9. Zone Plate coded image of α-emission from compressed D-T microsphere.

Fig. 10. α-particle imaging results. Target was 86 μm diameter D-T filled glass microsphere irradiated with 2.4×10^{12} watts at Argus.

Fig. 11. Schematic of Argus neutron time-of-flight spectrometer.

Fig. 12. Outline of neutron time-of-flight data analysis scheme.

Fig. 13. D-T neutron energy spectrum from Argus target experiment.

Fig. 14. Summary of some Argus neutron time-of-flight measurements and results.

Fig. 15. Comparison of the characteristics of the Argus and Shiva neutron time-of-flight spectrometers.

Fig. 16. Summary of current capability of laser fusion diagnostics.

TOPICS

Interferometry	(Attwood, Sweeney)
Zone Plate α-Imaging	(Ceglio)
Neutron Spectral Measurement	(Lerche)

40-90-0877-1893

FIG. 1

UV HOLOGRAPHIC INTERFEROMETER PROBE PULSE OPTICS

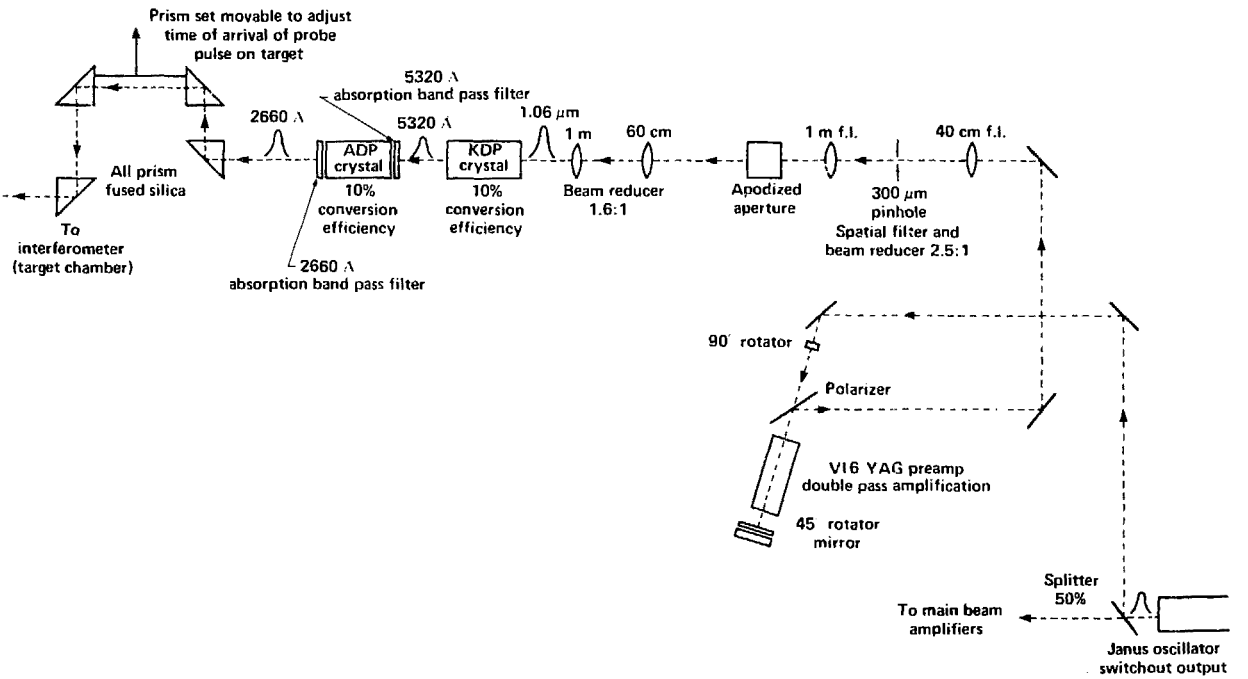

20-01-0877-1521

FIG. 2

UV HOLOGRAPHIC INTERFEROMETER TARGET CHAMBER SETUP

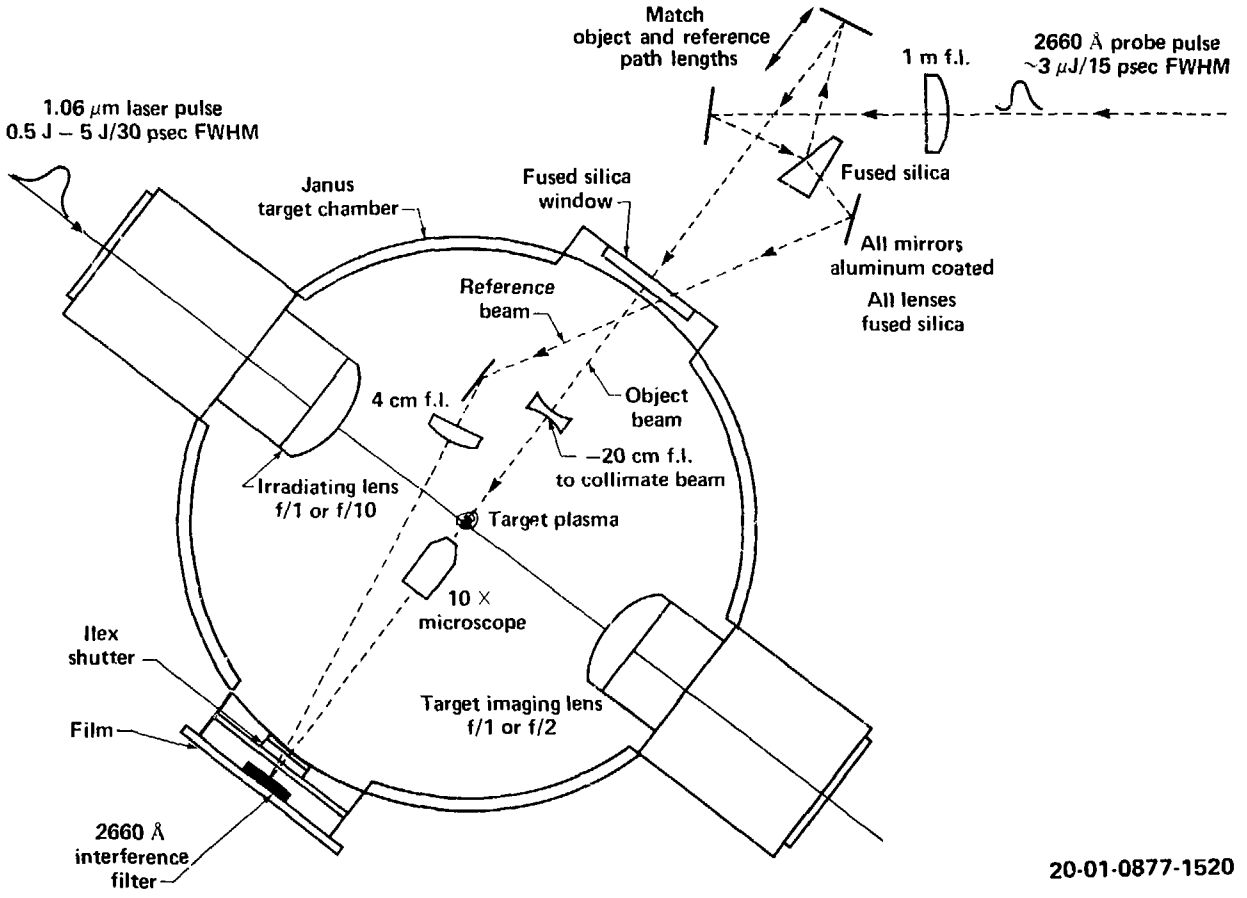

FIG. 3

PROFILE STEEPENING ON AXIS

(2660 Å, 15 psec, 1 μm)

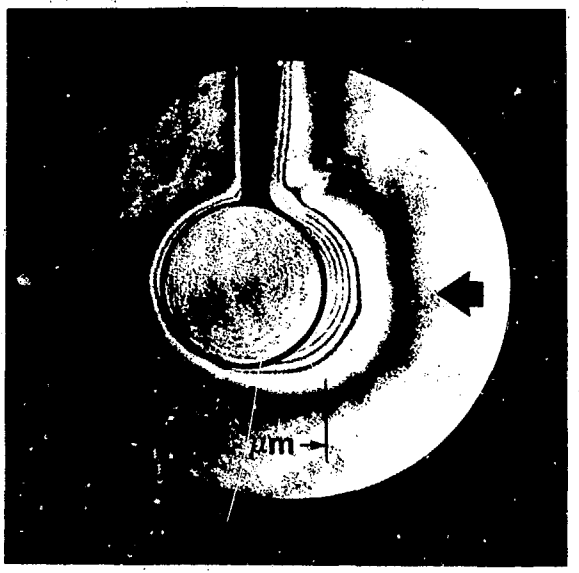

1.06 μm, ~10^{14} W/cm^2, 41 μm^D

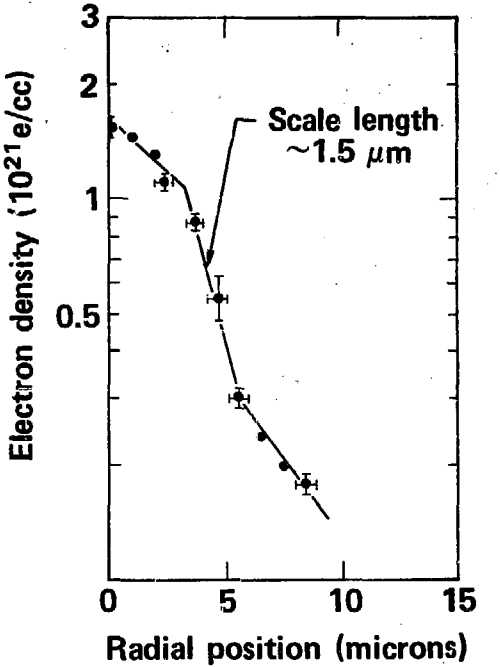

40-90-0877-1518

FIG. 4

FLAT DISK TARGETS

(2660 Å, 15 psec, 1 μm)

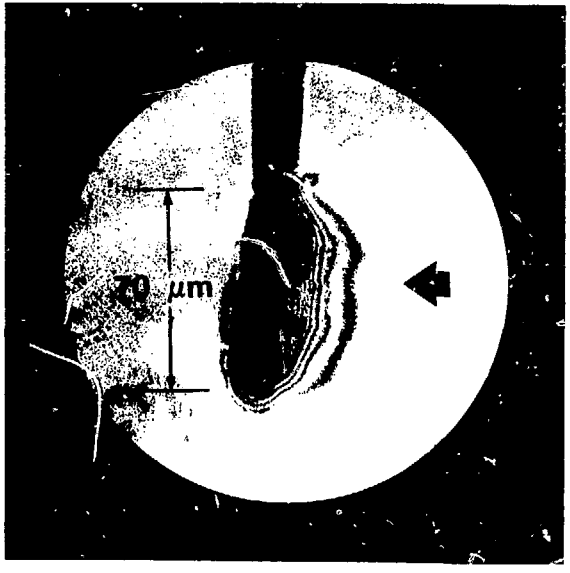

1.06 μm, ~10^{14} W/cm^2

A) Large scale cavity formation

B) Small scale surface rippling

C) Apparently faster contour velocities on axis

40-90-0877-1517

FIG. 5

ZONE PLATE CODED IMAGING (PRINCIPLES):

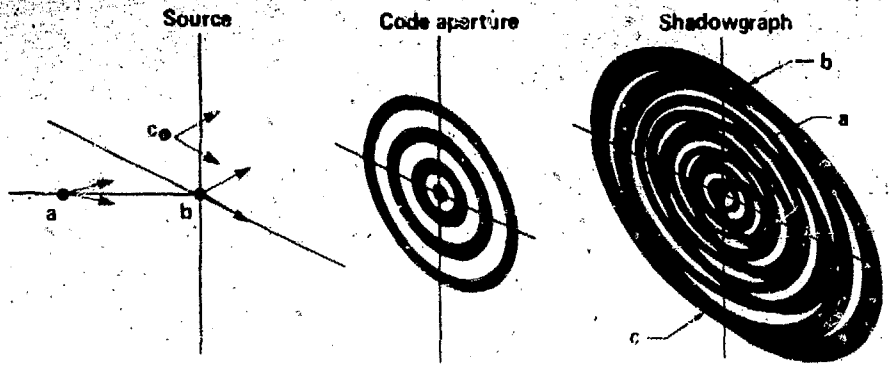

Each zone plate shadow uniquely characterizes the position of its associated source point

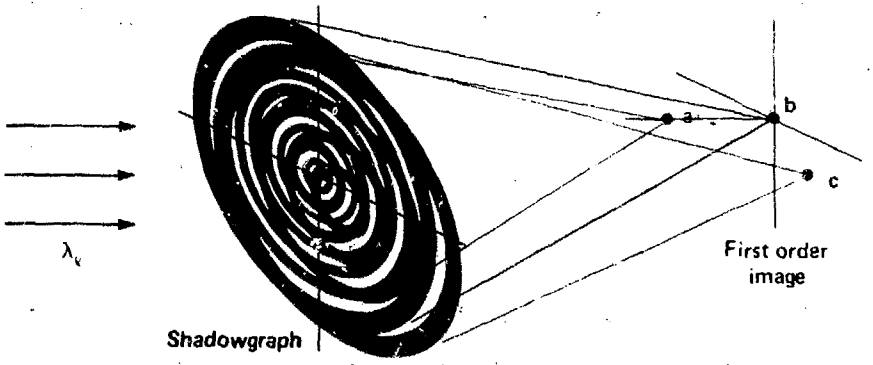

Original three dimensional source distribution is reconstructed from the shadowgraph

4/77

FIG. 6

ZPCI OF α-PARTICLE EMISSION FROM LASER COMPRESSED TARGETS

Technique:

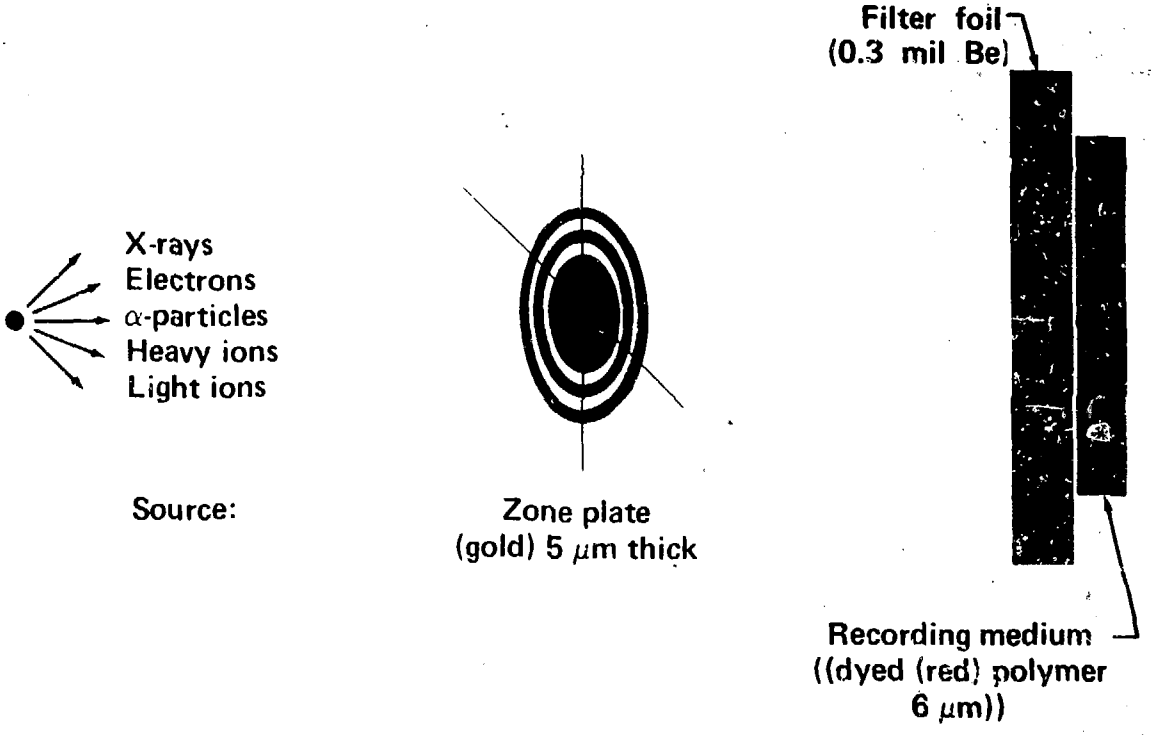

11/76

FIG. 7

LOGIC FOR RADIATION DISCRIMINATION IN ALPHA IMAGING EXPERIMENTS

1. Data appear as pinholes in the cellulose nitrate caused by radiations producing an ionization track all the way through the C.N. layer

---

2. X rays do not produce tracks

3. Electrons do not produce tracks

4. Heavy ions are stopped by the Be foil

5. Protons, deuterons, and tritons produce tracks only at low energy (.5; 1.0; 1.5 MeV) and at that energy they have a range in the C.N. significantly less than its 6 μm thickness.

---

6. Alphas emerging from the Be foil have appropriate energy to produce ionization tracks clear through the C.N.

5/77

FIG. 8

CODED IMAGE OF α EMISSION FROM COMPRESSED D-T MICROBALLOON

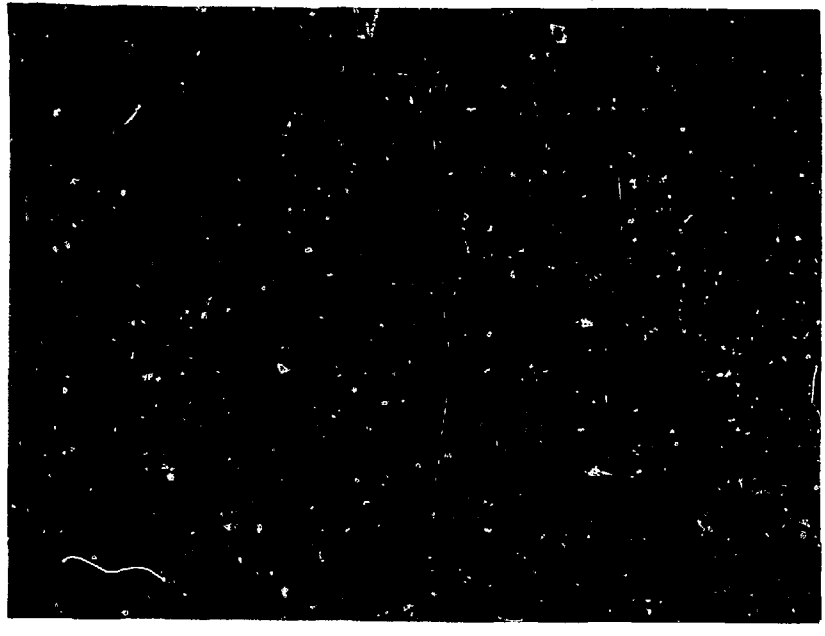

40-90-1176-2338

FIG. 9

ZONE PLATE CAMERA ALPHA IMAGING DATA: ABEL INVERTED

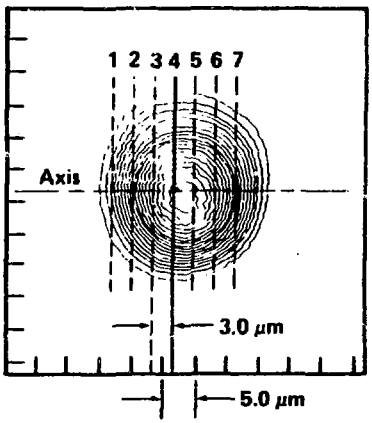

Reconstructed image
(isoemission contours)

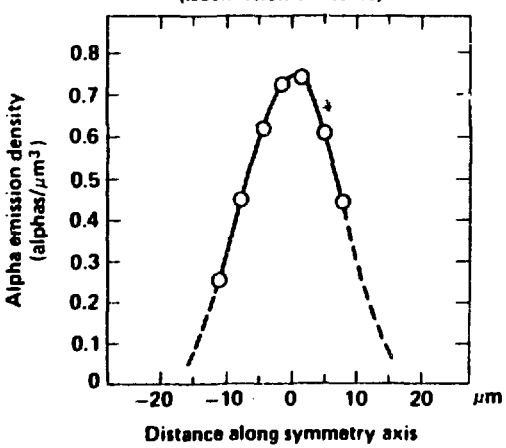

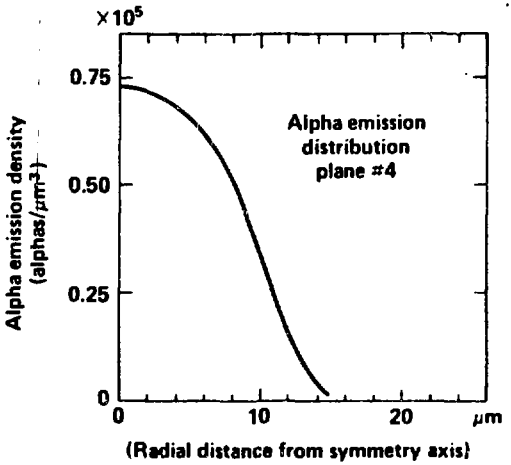

Shot parameters:

Target ball diameter: 86 μm
Power on target: 2.4×10^{12} watt
Neutron yield: 3×10^{8}
Shot I.D.: 36111611 RL-1-2

40-90-0877-1696

FIG. 10

NEUTRON TIME-OF-FLIGHT SPECTROMETER

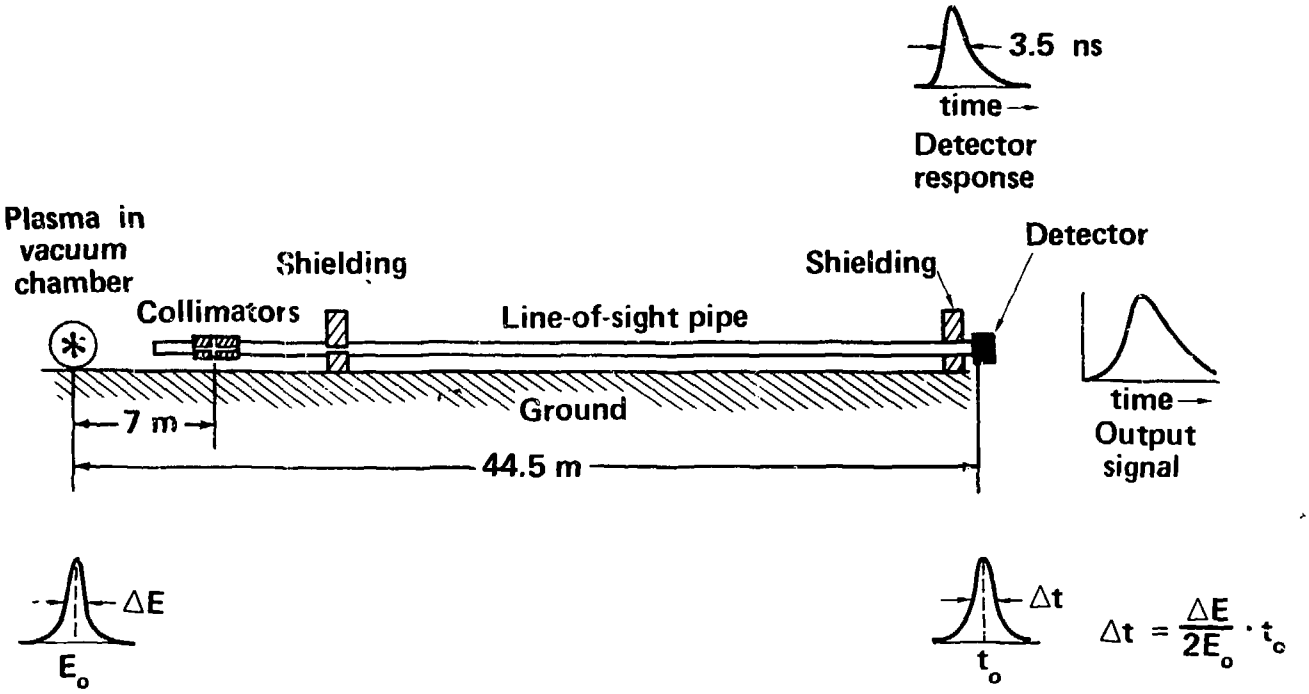

11/76

FIG. 11

NEUTRON TOF DATA ANALYSIS

1. Raw time domain data is recorded on oscilloscope.
2. Raw data is corrected for detector system time response with a computer code that uses an interative procedure.
3. Corrected time spectrum is converted to energy spectrum.
4. Energy spectrum is plotted as descrete points with error bars that represent neutron detection statistics.
5. Gaussian curve which gives best least squares fit to energy spectrum is determined.
6. D-T ion temperature is calculated from FWHM of Gaussian fit:

$$\Delta E = 177 \sqrt{T_i}$$

40-46-0877-1906

FIG. 12

DT-NEUTRON ENERGY SPECTRUM

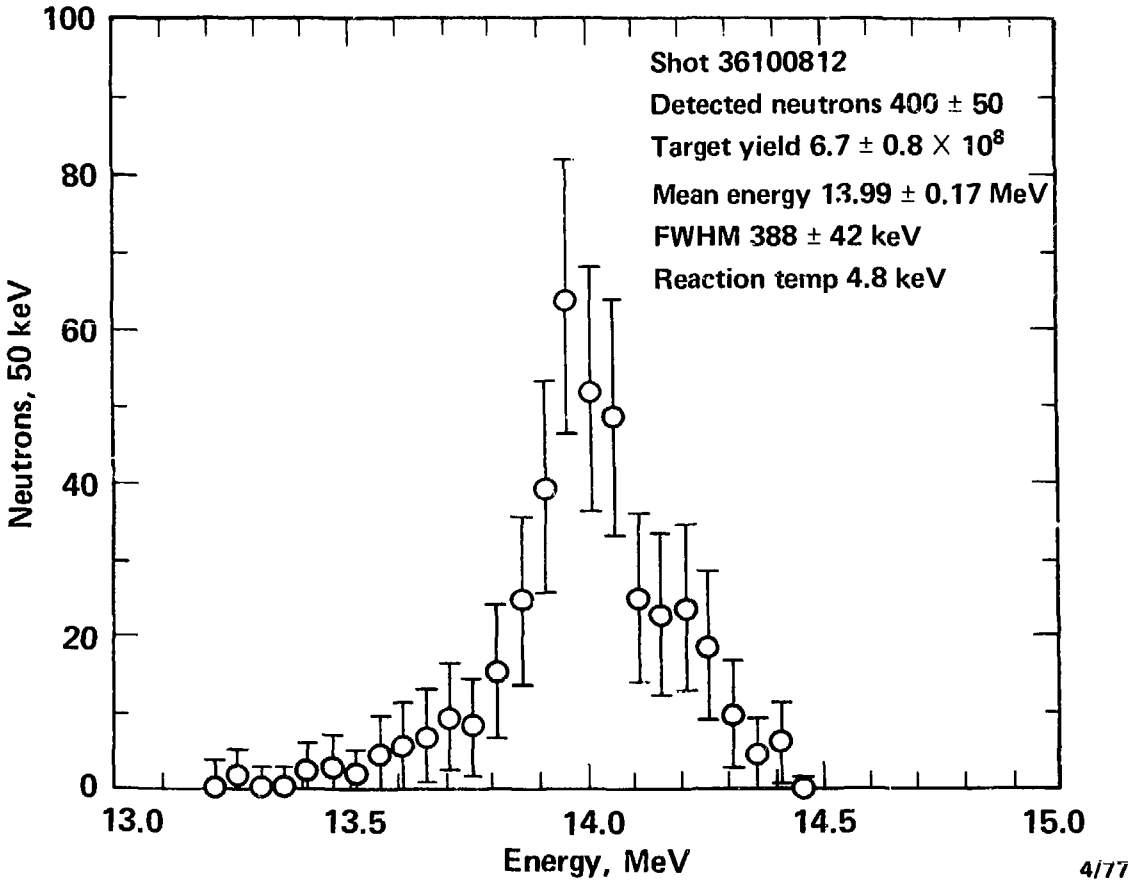

FIG. 13

SUMMARY OF NEUTRON TOF MEASUREMENTS AND CALCULATED ION TEMPERATURES. THE RESULT FOR EACH SHOT IS THE AVERAGE FOR TWO DETECTORS.

Shot	Neutron yield ($\times 10^8$)	Neutrons detected	Average neutron energy (MeV)	Energy width (keV)	Ion temperature (keV)
36092905	4.2 ± 1.0	250	13.98 ± 0.10	425	5.8 ± 1.3
36093003	6.0 ± 1.0	360	13.98 ± 0.10	405	5.2 ± 1.2
36100812	6.7 ± 0.9	410	14.00 ± 0.10	440	6.2 ± 1.3
36101202	3.3 ± 0.5	200	14.02 ± 0.10	385	4.7 ± 1.2
36101203	4.4 ± 0.6	270	14.02 ± 0.10	445	6.3 ± 1.3

40-46-0477-1172

7/77

FIG. 14

NEUTRON TOF SPECTROMETER CHARACTERISTICS

	Argus	Shiva
Flight path (meters)	44.5	125
Energy resolution (keV)	65	25
X-ray time of flight (ns)	149	417
D-T neutron time of flight (ns)	869	2441
Neutron transmission	0.94	0.32

Measurements on a plasma with an 8-keV ion temperature	Required neutron yield	
	Argus	Shiva
Ion temperature (± 2 keV)	2.1×10^8	4.9×10^9
Spectrum (65 keV)	1.6×10^9	3.7×10^{10}
Spectrum (25 keV)	—	1.1×10^{11}

40-46-0877-1725

FIG. 15

CURRENT STATUS OF LASER FUSION DIAGNOSTICS

Δt = 6 psec (infra-red)
= 15 psec (x-ray)
Δx = 1 μm (infra-red, visible, ultra violet; time integrated)
$\simeq$ 3 μm (x-ray; time integrated)
= 6 μm (x-ray; 15 psec time resolution)
= 50 μm (120 psec, full frame)
= 10 μm (α particles, ions)

$100\ \text{eV} \leqslant h\nu \leqslant 100\ \text{keV}$ (time integrated)
$1\ \text{keV} \leqslant h\nu \leqslant 20\ \text{keV}$ (15 psec time resolution)
$10^{16}\ \text{cm}^{-3} \leqslant n_e \leqslant 10^{21}\ \text{cm}^{-3}$ ($\approx$15 psec exposures)
$\Delta(h\nu) = 1\ \text{eV}$ at 1 keV
$\Delta E \simeq 100\ \text{keV}$ for 14 meV neutrons, 3.5 meV alphas

40-90-0377-1733 8/77

FIG. 16